On the Calculation of Supercritical Fluid−Solid Equilibria by Molecular Simulation

Simón Albo and Erich A. Müller*

Departamento de Termodinámica y Fenómenos de Transferencia, Universidad Simón Bolívar, Caracas 1080, Venezuela, and Departamento de Ciencias Ambientales, Universidad Pablo de Olavide, 41013 Sevilla, Spain

Received: September 2, 2002; In Final Form: November 26, 2002

Methods and intermolecular potentials apt for the molecular simulation of solubilities of solids in supercritical fluids are briefly reviewed. As an illustrative example, the solubilities of naphthalene in supercritical carbon dioxide at 328.15 K are studied using an isotropic multipolar potential model. Upon using the Widom insertion method, a quantitative prediction of the experimental data is obtained. A further look at the calculations shows that the customary implementation of the method is tainted by the use of experimental information about the vapor pressure and density of the solid. If the actual properties (obtained via simulation) of the model solid are used, the equilibrium is, in this example, poorly described. Full-scale molecular dynamic simulations, which include both the solid and fluid phases, confirm the results. It is shown how an accurate description and modeling of the solute solid-phase properties is a prerequisite for the determination of the solubilities of solids in supercritical fluids.

Introduction

Experimentally one encounters that in supercritical fluid (SCF) extraction processes the state of matter spans from solids below their triple point to fluids above their critical conditions, with a variety of state points and phases depending on the thermodynamic conditions of the mixture. The progress hitherto achieved using theoretical models has been invaluable both in understanding the phase equilibria and for correlating measured data. However, the quantitative description of solid−supercritical fluid equilibria poses a severe challenge to any model. For example, common cubic equations of state (EOS) will perform poorly if applied to predict simultaneously both the fluid-phase equilibria and the peculiar phenomena found in SCF−solid systems (e.g., the configurational properties of the solid phase, the large isothermal compressibility of the dense gas, the special interactions leading to liquid−liquid separations in the critical region, the large negative solution volumes of solids, etc). In this context, molecular simulation presents itself as a powerful tool with which to obtain physical insights on the underlying reasons for the observed and/or unexpected macroscopic behavior of fluids and materials since its outcome is independent of any theoretical approximations. In this sense, it is ever so more frequently used to understand both the equilibrium and transport processes of fluids. The challenge here is to describe the molecules with a suitable intermolecular potential function that is sufficiently detailed to predict the correct solid and fluid phase behavior and be simple enough to be amenable to a rapid solution by available hardware and/or software.

Although molecular modeling seems to be a promising route, care should be taken to perform the simulations in an appropriate manner to maintain the predictive power of the models. In this paper, we briefly review the algorithms available for studying SCF−solid thermodynamic equilibria and perform a simulation of a typical and well-studied test system, carbon dioxide−naphthalene, using accepted simulation algorithms. The results obtained using the most widely accepted algorithm (Widom insertion) show an apparent agreement with experimental data. However, upon further analysis, we have found the results to be very different from those obtained from "first principles" simulations that include simultaneously the solid and fluid phases. A close look at the inconsistency points to an erroneous (albeit unfortunately very common) inclusion of experimental data within the solution algorithm.

* To whom correspondence should be addressed. E-mail: emuller@usb.ve; emuller@dex.upo.es.

Simulation of SCF−Solid Equilibria

One may directly employ Monte Carlo (MC) [1,2] or molecular dynamics (MD) (e.g., refs 1,3−5) simulations of a dilute solute in a SCF to obtain specific information about the resulting monophase systems, particularly with regard to the equilibrium structure and solvation effects. However, if one does not incorporate implicitly or explicitly any information on the equilibrium solid phase, such simulation gives no information on the actual solubility. For this, one should in principle have both the fluid and solid phases in the same simulation box. This can naïvely be done by equilibrating a pure solvent and a pure solid separately and subsequently joining both simulation boxes. The system is then left to evolve by canonical dynamics, in much the same way as actual experimental batch solubility measurements are performed. Upon equilibration (which requires a diffusion of solid particles in the fluid phase), the fluid phase may be analyzed for both its composition and overall pressure. The simulations performed this way are extremely long (in terms of computer time) since equilibrium is driven by diffusion, a relatively slow process. Additionally, since solid solubilities are usually in the range of 100 ppm, system sizes may become prohibitively large. Such a situation has driven simulators to envision methods to speed up the process. Among the alternatives, one can (1) simplify the intermolecular potentials involved, noting that almost all of the computer time in a simulation is spent in the force calculations, (2) apply some alternative algorithm to short cut the actual full-scale simulation, or (3)

10.1021/jp026894m CCC: $25.00
Published on Web 01/24/2003

speed up the actual calculations (for example, using parallelism for MD calculations). We shall sequentially comment on these three aspects as applied to the simulation of a rather well-known test system, naphthalene−carbon dioxide, thus exemplifying the state-of-the-art options.

Isotropic Intermolecular Potential (IMP). The heart of any molecular simulation is the force field or intermolecular potential used. The reader is referred to general literature for complete reviews.[6,7] In general, a compromise must be made between the accuracy of the details to be included in the model and the computational cost associated with the energy calculation of a given force field. A detailed model is most likely to reproduce in a more satisfactory way a larger number of properties whereas a simpler one is generally more limited in scope and accuracy. One must bear in mind that more than three-fourths of the computer time of any fluid-phase simulation is consumed by energy and/or force calculations, and the computational effort typically rises on the order of $O(N^2)$, where N is the total number of molecules involved in the simulation. Thus, the potential models must be chosen appropriately with due consideration of the quality of the results desired and the hardware and algorithms available.

In a molecular dynamics calculation, the complexity of the potential model affects in a direct manner the computational effort required. For example, one of the most widely used models for the CO_2 molecule is the elementary physical model (EPM2) by Harris and Yung.[8] The EPM model is composed of three LJ spheres with partial charges associated with each atomic site (instead of an integrated central quadrupole) placed in such a way so as to produce a net quadrupole of $Q = -4.3 \times 10^{-26}$ esu (-1.43×10^{-39} C m^2). Within this model, the evaluation of interaction energies between two carbon dioxide molecules requires the calculation of $(3)^2$ site−site distances and, because of its nonsphericity, solving for the angular momentum conservation equations in each time step. Additionally, point charges require special computational techniques (e.g., Ewald summations) to account for the long-range interactions. One could simplify the intermolecular potentials by considering that a spherical geometry suffices for most calculations, particularly those involving high temperatures, where energetic effects presumably will dominate over entropic ones. By mapping the potential into a spherical model, one could decrease the computational effort by at least an order of magnitude of real time.

The simplest conceivable model consists of a sphere with both a single repulsion and attraction site. A typical potential, U_{ij}, of this type is the Lennard-Jones (LJ) potential and is given by

$$U_{ij}^{\mathrm{LJ}} = 4\epsilon_{ij}\left[\left(\frac{\sigma_{ij}}{r_{ij}}\right)^{12} - \left(\frac{\sigma_{ij}}{r_{ij}}\right)^{6}\right] \tag{1}$$

where σ and ϵ, the size and energy parameters, may be regressed from experimental data of several types, although no unique parameter set exists. Most common choices correspond to fits to viscosity data (Reid et al.,[9] $\sigma = 3.941$ Å; $\epsilon/k = 195.2$ K; Reed and Gubbins,[10] $\sigma = 4.018$ Å; $\epsilon/k = 194.7$ K) or from a direct fit to the critical temperature and density (Iwai et al.,[11] $\sigma = 3.912$ Å; $\epsilon/k = 225.3$ K; this work, $\sigma = 3.658$ Å; $\epsilon/k = 232.2$ K), from a fit to diffusion (Liu et al.,[12] $\sigma = 3.26192$ Å; $\epsilon/k = 500.71$ K), or from an overall fit to PvT properties (Iwai et al.,[13] $\sigma = 3.720$ Å; $\epsilon/k = 236.1$ K). Although it is well known that simple Lennard-Jones models (or for that matter, exp-6 models) do not adequately represent the potential surfaces of real molecules, the LJ model has been used extensively and successfully for the evaluation of phase equilibrium,[13−20] transport properties,[21−24] and adsorption[25] of supercritical CO_2 and mixtures. The model is simple and useful; however, it does not treat in an explicit fashion the nonspherical shape and the nonuniform charge distribution in the carbon dioxide molecule.

In the carbon dioxide molecule, the simplicity of being a small, rigid molecule is hampered by the presence of significant electrostatic effects, which make the problem of its description far from trivial. In general, multipolar interactions are angle-dependent, so one must specify both center-to-center distances and relative orientations for a proper evaluation of intermolecular potentials. If one performs an appropriate angle average,[10] one ends up with an angle-independent potential function that can be used in corresponding states correlations or, in our case, to obtain a simple isotropic multipolar potential (IMP) function, particularly

$$U_{ij}^{\mu\mu} = -\frac{\beta\mu_i^2\mu_j^2}{3r_{ij}^6} \tag{2}$$

$$U_{ij}^{\mu\mathrm{Q}} = -\frac{\beta(\mu_i^2Q_j^2 + Q_i^2\mu_j^2)}{2r_{ij}^8} \tag{3}$$

$$U_{ij}^{\mathrm{QQ}} = -\frac{7\beta Q_i^2Q_j^2}{5r_{ij}^{10}} \tag{4}$$

where the superscripts $\mu\mu$, μQ, and QQ refer to the dipole−dipole, dipole−quadrupole, and quadrupole−quadrupole interactions, respectively. Here, μ and Q are the dipole and quadrupolar moments, respectively. The resulting potential (i.e., the sum of eqs 1 and 2−4 is isotropic, i.e., is dependent only on the intermolecular distance). IMP is dependent on temperature T since $\beta = 1/kT$, where k is Boltzmann's factor. Thus, is it not truly a potential but rather an "effective" force field. Since all of our simulations are done at constant temperature, this does not present a problem.

Anticipating our use of the model for supercritical extraction processes, we chose to fit the critical point accurately, in detriment of the fit to other properties. For carbon dioxide, we have used a constant value of $\mu = 0$, $Q = -4.1 \times 10^{-26}$ esu[26] (-1.367×10^{-39} C m^2), $\epsilon/k = 215$ K; $\sigma = 3.748$ Å. The critical temperature predicted by IMP, obtained by finite-scale sizing calculations, is 304.8 ± 0.5 K, which compares well with the experimental value of 304.21 K. As a comparison, the corresponding result for the more complex EPM2 model is 302.5 ± 0.7 K. It is feasible that one could obtain different parameter values for the IMP model, which could produce a better fit of other properties of interest (e.g., densities, vapor pressures, etc). Alternatively, the value of the quadrupole moment might be varied, using it as a "tuning" parameter to produce a better modeling of a given property. The fit of IMP to the vapor−liquid temperature−density curve is observed in Figure 1, as compared to the results of a corresponding LJ fluid with parameters fitted to the critical temperature and density (without the quadrupole moment) and the EPM2 models. Although of slightly poorer performance than the more complex EMP2 model, since it underestimates the saturated vapor density and overestimates the liquid one, IMP captures the essential widening of the phase diagram due to the multipole moment. It is interesting that no matter what parameter set is chosen the LJ model alone is unable to follow the vapor−liquid curve adequately.

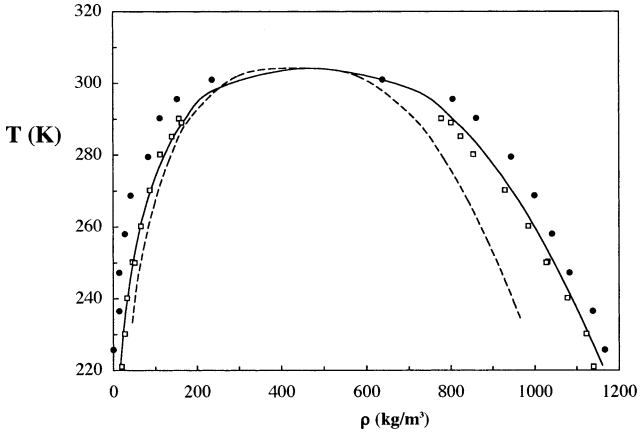

Figure 1. Saturated densities, ρ, for carbon dioxide as a function of temperature T. (—) Accurate reference equation of state,[27] (- -)Lennard-Jones equation of state[28] with parameters fit to corresponding states (σ = 3.658 Å; ϵ/k = 232.2 K), (□) EMP2 simulation results,[29] and (●) IMP potential.

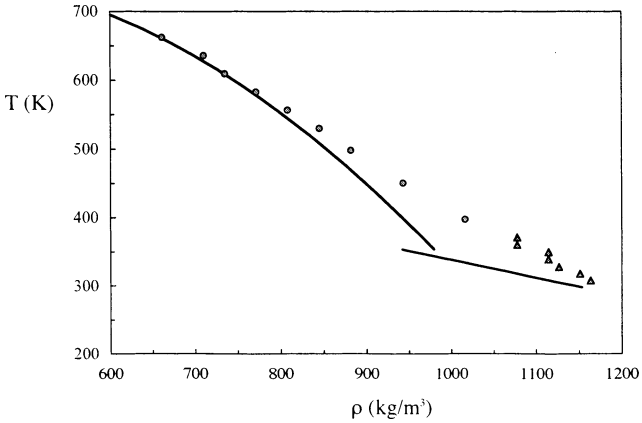

Figure 2. Saturated densities, ρ, for naphthalene as a function of temperature T. Gray circles and triangles are simulation results for liquid and solid naphthalene, respectively. Solid lines are the correlated experimental data.[30]

The sphericalization procedure employed to model CO_2 may be applied to other polar nonspherical molecules. As an example, we have studied naphthalene, a common test solute used in supercritical fluid extraction. Here, we have fit to the available saturated liquid-phase density data.[30] We used $\mu = 0$, $Q = 13.5 \times 10^{-26}$ esu[31] (4.503×10^{-39} C m^2), $\epsilon/k = 530$ K, and $\sigma = 5.5806$ Å. Figure 2 shows the quality of the fit as compared to the correlated experimental data of both the saturated liquid and solid. A pitfall of the IMP is seen at low temperatures, where structured phases may occur. Clearly, close-range repulsion and shape factors will be dominant in determining the structure and density at these conditions. In Figure 2, the largest deviations from experimental values are obtained at conditions close to the triple point, and the solid−fluid transition seems poorly determined.

Although the application of IMP to SCF−solid is somehow far-fetched considering it is an isotropic model, with no consideration for the actual shape of the molecules, it is an improvement over the LJ model. We chose to use it in this study to obtain some insight on its applicability.

Simulation Strategies. Apart from the naïve first principles or direct two-phase simulation approach, one has other simulation algorithms available. If a canonical simulation is set up with a solute composition that exceeds the solubility limit, then some clustering may be evident within the simulation cell. However, finite size effects make the determination of this clustering difficult. In too small a system, the simulation cell may stabilize in a metastable one-phase system. However, if one places a large enough system within the spinodal region (i.e., in a mechanically unstable situation), one obtains a phase separation. In this case, a supercritical fluid and a "precipitated" solid phase are observed. This is the essence of the temperature quench MD method (TQMD)[32] in which a homogeneous one-phase mixture (usually at an arbitrarily high temperature) is quenched at constant volume to the desired temperature. If the initial compositions are chosen correctly, then the system will phase separate within the simulation volume. Each of the resulting phases may be further analyzed in a separate fashion. The full evolution of the system into two regions separated by a planar interface is not necessary since compositions and densities stabilize in a relatively fast way. Suitable analysis of the clusters initially formed allows the determination of equilibrium phase compositions and densities. This method, however, produces metastable solid phases (usually amorphous solids) and is still not fully evaluated with respect to its capabilities.

The basis of most recent supercritical fluid solubility calculations using molecular simulation rests on the Widom insertion method,[33] known also as the potential distribution method or the test-particle method. This method allows the estimation of the chemical potential of a substance in a given fluid by examining the probability of the insertion of a supernumerary (called ghost or test) particle in an equilibrated fluid. The energy required for such an insertion is related to the work required to introduce the particle in the fluid (i.e., its chemical potential). Operationally, one must repeatedly attempt to place "ghost" solute particles into an equilibrated solvent, bookkeeping the energy of the "ghost" particle with the reamining particles.

If the solute system is kept under isobaric−isothermal conditions (thus volume is fluctuating), then the residual chemical potential of the solute, μ_2^{res}, is given by

$$\mu_2^{res} = -kT \ln\left[\frac{\langle V \exp(-U_2^{test}/kT)\rangle}{\langle V\rangle}\right] \tag{5}$$

where the quantities in brackets $\langle\ \rangle$ correspond to averages over all of the configurations of the fluid and U_2^{test} is the total interaction potential energy between the test particle and the solvent molecules. If the solvent system is kept under canonical conditions (constant density and temperature), then the corresponding equation is

$$\mu_2^{res} = -kT \ln\langle \exp(-U_2^{test}/kT)\rangle \tag{6}$$

however, the total pressure must be calculated as an ensemble average from the simulation itself.

Since the chemical potential of both components must be the same both in the fluid and in the solid phase, the following relation must hold:

$$\mu_i^{solid} = \mu_i^{fluid} \tag{7}$$

which in terms of fugacities is written as

$$\hat{f}_i^{solid} = \hat{f}_i^{fluid} \tag{8}$$

where the subscript i refers to the components in the mixture, the superscripts indicate the coexisting phases, and $\hat{f}_i$ refers to the fugacity of component i in a mixture. Upon making the assumption that the solvent is not present in the solid phase, the thermodynamic (diffusive) equilibrium condition for a binary

system corresponds to a single equation similar to eq 8 (for component 2). If we assume the solute to be present in small quantities, then we may consider the fugacity to be linearly dependent on the composition.

$$\hat{f}_i^{\text{fluid}} = H_2 y_2 \tag{9}$$

The slope of this straight line, Henry's constant, H_2, may be calculated at any (small) composition and is equal to the fugacity coefficient, $\hat{\phi}_2$, multiplied by the system pressure. It is most useful to evaluate it at infinite dilution (i.e., $y_2 \rightarrow 0$), where it is directly related to the residual chemical potential

$$H_2 = \rho_1 kT \exp\left(\frac{\mu_2^{\text{res}}}{kT}\right) \tag{10}$$

Additionally, the fugacity of the solid phase may be evaluated using standard thermodynamic relationships.

$$\hat{f}_2^{\text{solid}} = P_2^{\text{sat}} \exp\left[\frac{\upsilon_2^{\text{solid}}(P - P_2^{\text{sat}})}{kT}\right] \tag{11}$$

Finally, from eqs 8−11, the solubility is calculated from

$$y_2 = \frac{P_2^{\text{sat}}}{\rho_1 kT} \frac{1}{\exp(\mu_2^{\text{res}}/kT)} \exp\left[\frac{\upsilon_2^{\text{solid}}(P - P_2^{\text{sat}})}{kT}\right] = \frac{P_2^{\text{sat}}}{\rho_1 kT} \exp\left[\frac{\upsilon_2^{\text{solid}}(P - P_2^{\text{sat}}) - \mu_2^{\text{res}}}{kT}\right] \tag{12}$$

This procedure has been employed for modeling solubilities of solutes in supercritical CO_2 using both NPT[34−37] and NVT[13,38−43] Monte Carlo simulations.

To evaluate eq 12, one should obtain from a suitable model (a) ρ_1, the pure solute density at a given pressure and temperature, (b) μ_2^{res}, the residual chemical potential of the solute in the solvent at infinite dilution, and (c) $1/\upsilon_2^{\text{solid}}$, the density and P_2^{sat}, the vapor pressure of the saturated solid. Rigorously, all of these properties must be obtained for the *same* model. Both the solute density (a supercritical fluid at the given P and T) and the residual chemical potential may be obtained with relatively modest effort using relatively small simulation cells and short runs. However, obtaining the vapor pressure and solid saturated volume of the solute model by simulation requires considerable computational effort, basically resolving the solid−fluid equilibria of the pure solute. To circumvent this problem, it is universally accepted that the *experimental* values of P^{sat} and υ^{solid} should be employed.

All algorithms based on the Widom insertion technique are constrained with respect to the density of the solvent and with respect to the size and shape of the solute. This method is applicable only if the fluid density is not too large; otherwise, the insertion probability will be too low and the statistics poor. In many cases, the practical upper density limit coincides with that encountered in typical supercritical extraction processes, namely, between 1 and 2 times the solvent critical density. Typically, the shape and size of supercritical solutes is large, their molecular weight exceeding in many cases that of the solvent by an order of magnitude. Under these circumstance, the possibility of encountering a suitable "cavity" within the fluid to insert a solute molecule is extremely low. Even with the use of configurational-bias techniques,[44,45] the statistics may be poor.

Other available techniques include grand canonical Monte Carlo[46] simulations, the Kirkwood coupling method,[47] Gibbs−Duhem integration, [48−50] the virtual Gibbs ensemble,[51] and integral equation methods.[52,53] Of these, the simplest and by far least demanding from a computational point of view are the methods based on Widom insertion. We have performed the molecular modeling of our test system using the Widom method (i.e., via the use of eq 12), as is commonly implemented, and have compared the results with the simulation of the same system via direct MD methods.

Simulation and Hardware Issues. The rate at which one obtains results via molecular simulation is directly proportional to the actual processor speed. Apart from using a state-of-the-art processor, one may attempt to parallelize the calculations to obtain significant increases in speed. MD calculations are especially suited for this type of approach (as opposed to MC-based methods). For recent reviews of the parallelization schemes in MD, the reader is referred to Plimpton[54] and Heffelfinger.[55]

In our simulations, we have used canonical (constant density and temperature) MD calculations. We have used a fifth-order Gear predictor−corrector algorithm[56] to solve the equations of motion. Constant temperature is obtained with the Nosé-Hoover[57,58] thermostating method in which the total kinetic energy of the system is coupled to an external degree of freedom ensuring a canonical distribution of momenta. The program is parallelized using a domain-decomposition approach in which a rectilinear volume is assigned to each processor in a 3D decomposition scheme. The MPI library is used for interprocessor communication. A cluster of five machines (one master and four workers) along with a 2 MB/s Myrinet communication switch was used for these calculations.

We have performed simulations using the Widom insertion method (i.e., using eq 6 to obtain the residual chemical potential necessary to evaluate eq 12). For this purpose, we set up canonical molecular dynamics simulations at 328.15 K and densities that give the corresponding pressures. We used cubic simulation cells with 10 000 carbon dioxide particles. Once the system was equilibrated, after 300 fs of system evolution, 1000 insertions were attempted for a total of 0.75 ns of production time (a total of 2.5×10^6 insertion attempts per state point). From simulations, the values of the infinite dilution residual chemical potential are readily obtained.

The IMP potentials are short-ranged, so in finite size simulations, a cutoff of the potential is applied. In our case, we have used a cutoff radius of 4 times the characteristic length scale of the CO_2 molecule. For the cross-interaction terms, the customary Lorentz−Berthelot mixing rules have been applied, $\sigma_{ij} = 0.5(\sigma_{ii} + \sigma_{jj})$ and $\epsilon_{ij} = (\epsilon_{ii}\epsilon_{jj})^{0.5}$, and no binary adjustable parameters have been considered.

Full-scale simulations were performed using canonical dynamics, placing an equilibrated solid and a fluid in the same simulation box and letting the system evolve in time. We have used systems of up to 64 000 molecules and have spanned a wide range of compositions. For visualization purposes, we report in detail here a simulation of a relatively small system of 3336 naphthalene molecules placed initially in a structured solid configuration. The simulation box is initially filled with 400 particles of carbon dioxide in a fluid state to give the desired overall density.

Results

For the evaluation of eq 12, one needs to obtain the vapor pressure and density of the solid (naphthalene). If along with

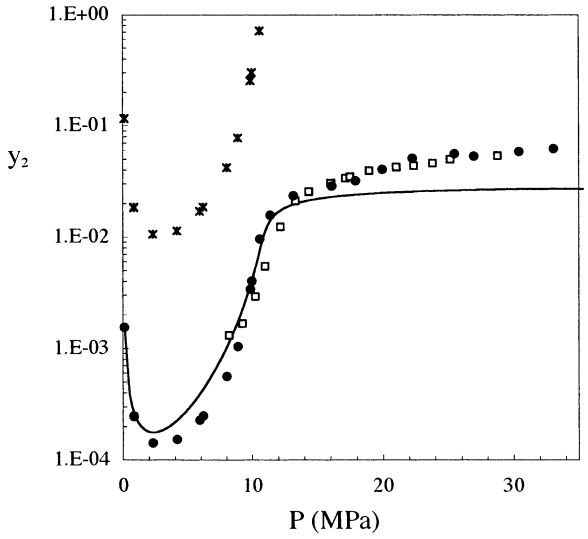

Figure 3. Solubility, y_2, of naphthalene in supercritical CO_2 at 328.15 K. (□) Experimental data[59] and (—) the correlation using the Peng−Robinson EOS. Other symbols are simulations using experimental (●) and model (×) values of the naphthalene vapor pressure and solid density.

the simulation results for the fluid density and residual chemical potential we employ the experimental values $P^{sat} = 160$ Pa and $v^{sat} = 1.25 \times 10^{-4}$ m^3/mol, then we obtain the results shown in Figure 3 (solid circles). The results show a remarkable similarity to the experimental data. The most striking feature is the lack of any adjustment of the binary mixture (i.e., no binary interaction parameters have been used), so the result is apparently a prediction of mixture properties from the fit of pure component data. The simulation data follow the correct experimental trends and actually extend the range of the data involved.

For comparison purposes, in Figure 3 the prediction of the Peng−Robinson EOS is also plotted. The equilibrium here is solved in a manner analogous to the simulation method (for a complete description, see ref 60). The residual chemical potential calculation is substituted for a term involving the fugacity coefficient of the solute in the solvent at the given temperature, pressure, and composition (therefore, the solution procedure is iterative). In much the same way as in the simulations, the solid saturation properties are needed, and in the same way, the use of experimental values is the accepted norm. The quality of the fit without the use of binary interaction parameters is fair; there are some differences with the experimental data, especially at high pressures. The results may be improved by using a larger number of fitting parameters, and several schemes[61] are available for this purpose.

The apparent agreement between the simulations and the data is, however, fortuitous. If one takes the molecular model and calculates by simulation the saturation properties of pure naphthalene, then one obtains values that differ from the experimental values in very significant ways. We used a cubic simulation cell with 2905 naphthalene molecules and equilibrated a solid phase at 328.15 K at a pressure of roughly 1 atm. After equilibration, one side of the simulation box (initially a cube) was expanded 50-fold, leaving a parallelepiped with a large amount of void space (i.e., the simulation cell was left with a small slab of solid surrounded by large amounts of void space). The resulting system is left to evolve with canonical MD, a process similar to the TQMD. The system attains equilibrium in a rather fast way. After 4 ns of equilibration, we took averages of the vapor density for 20 ns, obtaining a vapor pressure of 10.2 ± 1.5 kPa and a solid volume of $v^{sat} = 1.13 \pm 0.05 \times 10^{-4}$ m^3/mol. The vapor pressure is significantly different than the experimental value. Using these model values and replotting the solubility, one obtains a solubility curve (crosses) that is shifted upward in Figure 3. In fact, such a result suggests an infinite solubility in much of the range of the pressures of interest.

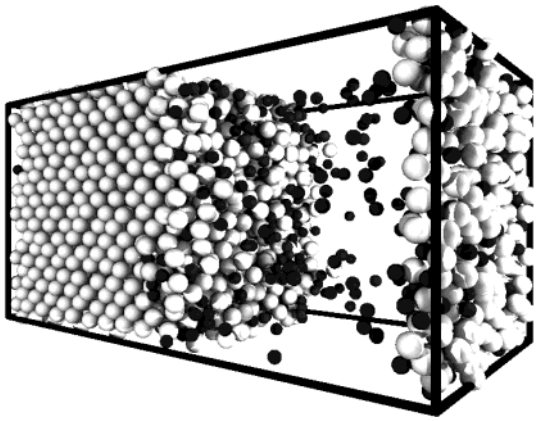

Figure 4. Snapshot of a configuration at 328.15 K after 220 ns from direct MD simulations. White spheres are naphthalene, and black spheres are carbon dioxide. The starting point is a slab of pure solid naphthalene in contact with fluid carbon dioxide.

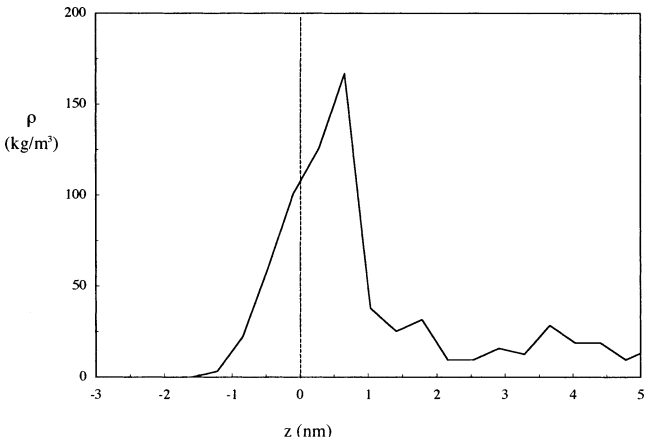

Figure 5. Carbon dioxide density profile in the direction normal to the solid−fluid interface. The dashed line is a guide to the eye corresponding to the approximate position of the interface. Other simulations details are the same as in Figure 4.

Figure 4 is a snapshot of a direct simulation for the system at a total pressure of 1.0 ± 0.1 MPa after 220 ns. It is possible that real diffusion times for these systems are longer than the time scales studied. However, the configuration seemed stable and unchanging for most of the simulation time. Figure 5 shows the average solute density profiles for a final configuration. The adsorption at the solid−fluid interface is apparent and worth noting. It is attained rapidly within the simulation. Both the roughness of the solid phase and the low fluid densities preempt the formation of a thick wetting film.

No diffusion into the solid is observed (i.e., the assumption of a "pure" solid phase, implicit in eq 12, is apparently correct, even for this extreme case in which the overall solubilities are high). The system corresponds to a fluid composition of $y_2 = 0.018 \pm 0.005$ and a pressure of 1.0 ± 0.1 MPa, which agree with the estimates obtained by using the Widom insertion method and the model solid properties (i.e., crosses in Figure 1). At other conditions, namely, pressures above 10 MPa, one observes that indeed, as predicted by the Widom insertion method using the model solid properties, the system exhibits

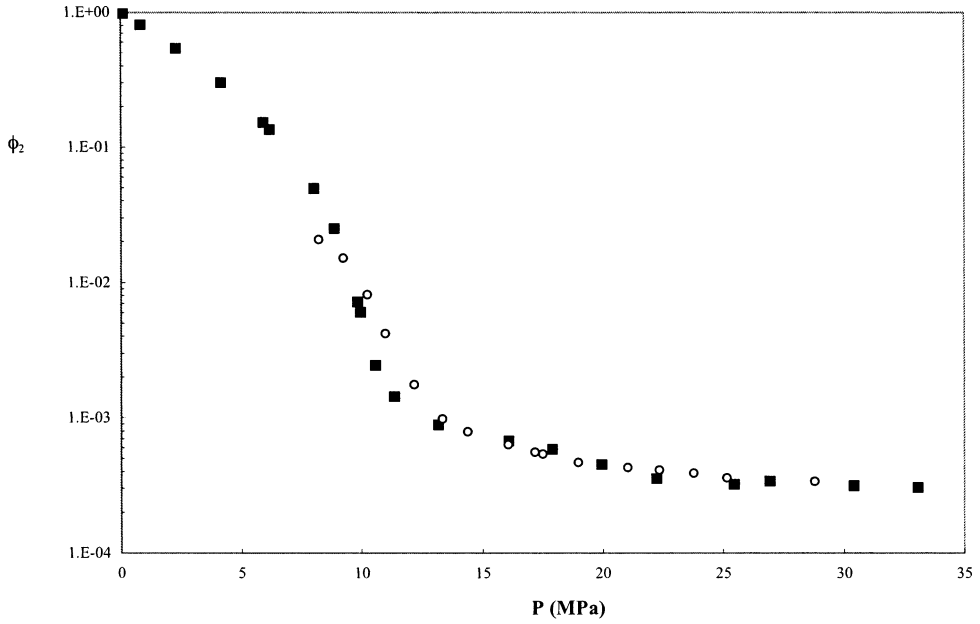

Figure 6. Fluid-phase fugacity coefficients, $\hat{\phi}_2$, of naphthalene in supercritical CO_2 at 328.15 K as a function of pressure. Simulation data (■) (eq 13) and experimental data (○) (eq 14).

complete miscibility (i.e., the fluid phase is capable of dissolving an infinite amount of solute).

In any case, it is evident that the parameter values employed, and possibly even the model itself, are incapable of correctly describing the behavior of the solid in spite of the apparent success shown in Figure 3. The root of the problems is apparently the inability of the model to describe both the equilibrium (vapor pressures) and energetic (enthalpies of sublimation) properties of the solid correctly. The fit of two model parameters to saturated liquid densities, although sufficient to obtain a suitable model for vapor−liquid and/or liquid−liquid equilibria, is not enough for solid−fluid calculations. The danger here is that if one believes, by observing the apparent coincidence between the model and experiments shown by the circular symbols in Figure 3, that the molecular model is correct then one is tempted to employ the model to obtain other properties (e.g. diffusion coefficients, kinetics, equilibria, etc). The results of this practice are bound to give erroneous results since the physics of the problem is incorrect. Unfortunately, the latter has been standard practice.

One may be tempted to compare the corresponding Henry constants from both simulation and experimental results. This procedure, which is equivalent to comparing fluid-phase fugacity coefficients,[52] consists of comparing the results of

$$[\hat{\phi}_2]_{\text{simulation}} = \frac{\rho_1 kT}{P} \exp\left(\frac{\mu_2^{\text{res}}}{kT}\right) \tag{13}$$

where all terms on the RHS are obtained from a fluid simulation (i.e., using Widom insertion) to the results of

$$[\hat{\phi}_2]_{\text{exptl}} = \left(\frac{P_2^{\text{sat}}}{y_2 P}\right) \exp\left[\frac{v_2^{\text{solid}}(P - P_2^{\text{sat}})}{kT}\right] \tag{14}$$

(cf. eq 11) which can be evaluated directly from experimental data. This allows for a comparison of the ability of the intermolecular potential to model the fluid-phase solvation that is, however, a necessary but not sufficient condition to model the solid−fluid equilibria. A comparison for the model case is shown in Figure 6, where agreement is observed between the IMP potential and the experiments, despite the poor performance of the molecular model in describing the actual equilibrium.

Conclusions

Of all of the simulation methods available, the simplest and by far least demanding from a computational point of view are the methods based on Widom insertion. They have severe constraints with respect to the complexity and size of the solute and with respect to the density of the solvent. However, if applicable, they allow the calculation of the solubilities of solids in SCF with relative ease. Particularly, if simple (isotropic) potentials are involved and/or parallel computer processing employed, then calculations may be performed in a few hours.

However, extreme care should be taken to avoid the severe inconsistencies that arise from mixing in the same equations for calculating solubilities for the *experimental* data for the solid phase along with the simulation results. In these particular types of calculations, the solid phase is represented by a molecular model for which the thermodynamic properties must be evaluated by simulation. Should the ultimate objective be the correlation of experimental data using a simple model, the use of experimental vapor pressures (and to a lesser degree experimental solid densities) in equations similar to eq 12 might be justified. In these cases, an accurate correlation may be obtained, and the available experimental data may be sensibly extrapolated. It is important to note that this practice does not constitute an appropriate simulation of the molecular model. By effectively ignoring the properties of the model solid, the overall physics of the system is lost, and any conclusions that transcend the correlation may be severely in error. We strongly make the point that it is not the Widom insertion method that failed in the example given here but was rather due to the poor choice (for this application) of the intermolecular potential.

Spherical models such as LJ or IMP are unsuitable for studying solid−fluid phenomena since no proper account is taken for the actual structural properties of the solid. A search should be made, particularly in the case of the solute, for more detailed models that reproduce the solid density and vapor pressure with some degree of accuracy.

Direct canonical (constant density and temperature) simulation of two-phase solid−fluid systems, once disregarded as a slow

and computationally prohibitive method, is currently a viable option mainly because of the availability of parallel versions of molecular dynamics programs and ever-increasing processor speeds.

Acknowledgment. E.A.M. thanks Professor Lev Gelb for ongoing discussions on the topic and for allowing us to employ the lj2_dist (v.14) program suite that has been used throughout this work. All simulations have been carried out at the Laboratorio de Computación de Alto Rendimiento, Universidad Simón Bolívar with funding from Fonacit/Agenda Petroleo (project 97-003530).

References and Notes

(1) Nakanishi, K. *Fluid Phase Equilib.* **1998**, *144*, 217.
(2) Zhang, X.; Gao, L.; Liu, Z.; He, J.; Zhang J.; Han B. *J. Supercrit. Fluids* **2002**, *23*, 233.
(3) Zhou, J.; Lu, X.; Wang, Y.; Shi, J. *Fluid Phase Equilib.* **2000**, *172*, 279.
(4) Inomata, H.; Saito, S.; Debenedetti, P. G. *Fluid Phase Equilib.* **1996**, *116*, 282.
(5) Salaniwal, S.; Cui, S. T.; Cochran, H. D.; Cummings, P. T. *Langmuir* **2001**, *17*, 1773, 1784.
(6) Leach, A. R. *Molecular Modelling*; Longman: Essex, U.K., 1997.
(7) Price, S. L. *Rev. Comput. Chem.* **2000**, *14*, 225.
(8) Harris, J. G.; Yung, K. H. *J. Phys. Chem.* **1995**, *99*, 12021.
(9) Prausnitz, J. M.; Poling, B. E.; O'Connell, J. P. *The Properties of Gases and Liquids*, 5th ed.; McGraw-Hill, New York, 2000.
(10) Reed, T. M.; Gubbins K. E. *Applied Statistical Mechanics*; Butterworth-Heinemann, Stoneham, 1973.
(11) Iwai, Y.; Uchida, H.; Arai, Y.; Mori, Y. *Fluid Phase Equilib.* **1998**, *144*, 233.
(12) Liu, H. Q.; Silva, C. M.; Macedo, E. A. *Ind. Eng. Chem. Res.* **1997**, *36*, 246.
(13) Iwai, Y.; Koga, Y.; Hata, Y.; Uchida, H.; Arai, Y. *Fluid Phase Equilib.* **1995**, *104*, 403.
(14) Iwai, Y.; Uchida, H.; Koga, Y.; Mori, Y.; Arai, Y. *Fluid Phase Equilib.* **1995**, *111*, 1.
(15) Iwai, Y.; Uchida, H.; Koga, Y.; Arai, Y.; Mori, Y. *Ind. Eng. Chem. Res.* **1996**, *35*, 3782.
(16) Koga, Y.; Iwai, Y.; Yamamoto, M.; Arai, Y. *Fluid Phase Equilib.* **1997**, *131*, 83.
(17) Nakanishi, K. *Fluid Phase Equilib.* **1998**, *144*, 217.
(18) Yamamoto, M.; Iwai, Y.; Arai, Y. *Fluid Phase Equilib.* **1999**, *163*, 165.
(19) Iwai, Y.; Mori, Y.; Arai, Y. *Fluid Phase Equilib.* **2000**, *167*, 33.
(20) Guo, M. X.; Lu, B. C. Y. *Thermochim. Acta* **1997**, *297*, 187.
(21) Iwai, Y.; Higashi, H.; Uchida, H.; Arai, Y. *Fluid Phase Equilib.* **1997**, *127*, 251.
(22) Higashi, H.; Iwai, Y.; Uchida, H.; Arai, Y. *J. Supercrit. Fluids* **1998**, *13*, 93.
(23) Higashi, H.; Iwai, Y.; Arai, Y. *Ind. Eng. Chem. Res.* **2000**, *39*, 4567.
(24) Zhou, J.; Lu, X.; Wang, Y.; Shi, J. *Fluid Phase Equilib.* **2000**, *172*, 279.
(25) Nitta, T.; Shigeta, T. *Fluid Phase Equilib.* **1998**, *144*, 245.
(26) Buckingham, A. D. *Q. Rev.* **1959**, *13*, 183.
(27) Bender, E. *Proc. Symp. Thermophys. Prop.* **1970**, *5*, 227.
(28) Johnson, J. K.; Zollweg, J. A.; Gubbins, K. E. *Mol. Phys.* **1993**, *78*, 591.
(29) Vorholz, J.; Harismiadis, V. I.; Rumpf, B.; Panagiotopoulos, A. Z.; Maurer G. *Fluid Phase Equilib.* **2000**, *170*, 203.
(30) Daubert, T. E.; Danner, R. P. *Physical and Thermodynamic Properties of Pure Chemicals;* National Standard References Data System (NSRDS); AIChE: New York, 1992.
(31) Gray, C. G.; Gubbins, K. E. *Theory of Molecular Fluids—Volume 1: Fundamentals*; Clarendon Press: Oxford, U.K., 1984.
(32) Gelb, L. D.; Müller, E. A. *Fluid Phase Equilib.* **2002**, *203*, 1.
(33) Widom, B. *J. Chem. Phys.* **1963**, *39*, 2808.
(34) Shing, K. S.; Chung, S. T. *J. Phys. Chem.* **1987**, *91*, 1674.
(35) Agrawal, P. M.; Rice, B. M.; Sorescu, D. C.; Thompson, D. L. *Fluid Phase Equilib.* **2001**, *187*, 139.
(36) Agrawal, P. M.; Sorescu, D. C.; Rice, B. M.; Thompson, D. L. *Fluid Phase Equilib.* **1999**, *155*, 177.
(37) Agrawal, P. M.; Rice, B. M.; Sorescu, D. C.; Thompson, D. L. *Fluid Phase Equilib.* **1999**, *166*, 1.
(38) Eya, H.; Iwai, Y.; Fukuda, T.; Arai, Y. *Fluid Phase Equilib.* **1992**, *77*, 39.
(39) Iwai, Y.; Koga, Y.; Hata, Y.; Uchida, H.; Arai, Y. *Fluid Phase Equilib.* **1995**, *104*, 403.
(40) Iwai, Y.; Uchida, H.; Koga, Y.; Mori, Y.; Arai, Y. *Fluid Phase Equilib.* **1995**, *111*, 1.
(41) Iwai, Y.; Uchida, H.; Koga, Y.; Arai, Y.; Mori, Y. *Ind. Eng. Chem. Res.* **1996**, *35*, 3782.
(42) Koga, Y.; Iwai, Y.; Yamamoto, M.; Arai, Y. *Fluid Phase Equilib.* **1997**, *131*, 83.
(43) Iwai, Y.; Mori, Y.; Arai, Y. *Fluid Phase Equilib.* **2000**, *167*, 33.
(44) Laso, M.; de Pablo, J.; Suter U. *J. Chem. Phys.* **1992**, *97*, 2817.
(45) Mooij, G.; Frenkel, D.; Smit, B. *J. Phys.: Condens. Matter* **1992**, *4*, L255.
(46) Nouacer, M.; Shing, K. S. *Mol. Simul.* **1989**, *2*, 55.
(47) Shing, K. S.; Chung, S. T. *J. Phys. Chem.* **1987**, *91*, 1674.
(48) Kofke D. A. *Mol. Phys.* **1993**, *78*, 1331.
(49) Kofke, D. A. *J. Chem. Phys.* **1993**, *98*, 4149.
(50) Lamm, M. H.; Hall, C. K. *Fluid Phase Equilib.* **2002**, *194*, 197.
(51) Shetty, R.; Escobedo, F. *J. Chem. Phys.* **2001**, *116*, 7957.
(52) Tom, J. W.: Debenedetti, P. G. *Ind. Eng. Chem. Res.* **1993**, *32*, 2118.
(53) Tanaka, H.; Nakanishi, K. *Fluid Phase Equilib.* **1994**, *102*, 107.
(54) Plimpton, S. *J. Comput. Phys.* **1995**, *117*, 1.
(55) Heffelfinger, G. S. *Comput. Phys. Commun.* **2000**, *128*, 219.
(56) Allen, M. P., Tildesley, D. J. *Computer Simulation of Liquids*; Clarendon Press: Oxford, U.K., 1987.
(57) Nosé, S. *Mol. Phys.* **1984**, *52*, 255.
(58) Hoover, W. G. *Phys. Rev. A* **1985**, *31*, 1695.
(59) McHugh, M.; Paulaitis, M. E. *J. Chem. Eng. Data* **1980**, *25*, 326.
(60) Tester, J. W.; Modell, M. *Thermodynamics and Its Applications*, 3rd ed.; Prentice-Hall: Upper Saddle River, NJ, 1997.
(61) Ashour, I.; Almehaideb, R.; Fateen, S.-E.; Aly, G. *Fluid Phase Equilib.* **2000**, *167*, 41.